Received 13 September 2016
Revised 30 May 2017
27 July 2017
Accepted 30 July 2017

Design of material microstructures for maximum effective elastic modulus and macrostructures

Daicong Da and Xiangyang Cui
State Key Laboratory of Advanced Design and Manufacturing for Vehicle Body, Hunan University, Changsha, PR China and Joint Center for Intelligent New Energy Vehicle, Shanghai, PR China

Kai Long
State Key Laboratory for Alternate Electrical Power System with Renewable Energy Sources, North China Electric Power University, Beijing, PR China, and

Guanxin Huang and Guangyao Li
State Key Laboratory of Advanced Design and Manufacturing for Vehicle Body, Hunan University, Changsha, PR China and Joint Center for Intelligent New Energy Vehicle, Shanghai, PR China

Abstract

Purpose – In pure material design, the previous research has indicated that lots of optimization factors such as used algorithm and parameters have influence on the optimal solution. In other words, there are multiple local minima for the topological design of materials for extreme properties. Therefore, the purpose of this study is to attempt different or more concise algorithms to find much wider possible solutions to material design. As for the design of material microstructures for macro-structural performance, the previous studies test algorithms on 2D porous or composite materials only, it should be demonstrated for 3D problems to reveal numerical and computational performance of the used algorithm.

Design/methodology/approach – The presented paper is an attempt to use the strain energy method and the bi-directional evolutionary structural optimization (BESO) algorithm to tailor material microstructures so as to find the optimal topology with the selected objective functions. The adoption of the strain energy-based approach instead of the homogenization method significantly simplifies the numerical implementation. The BESO approach is well suited to the optimal design of porous materials, and the generated topology structures are described clearly which makes manufacturing easy.

Findings – As a result, the presented method shows high stability during the optimization process and requires little iterations for convergence. A number of interesting and valid material microstructures are obtained which verify the effectiveness of the proposed optimization algorithm. The numerical examples adequately consider effects of initial guesses of the representative unit cell (RUC) and of the volume constraints of solid materials on the final design. The presented paper also reveals that the optimized microstructure obtained from pure material design is not the optimal solution any more when considering the specific macro-structural performance. The optimal result depends on various effects such as the initial guess of RUC and the size dimension of the macrostructure itself.

Engineering Computations
Vol. 35 No. 2, 2018
pp. 622-640

0264-4401
DOI 10.1108/EC-09-2016-0323

This work was supported by the National Science Foundation of China (11472101), Postdoctoral Science Foundation of China (2013M531780) and State Key Program of National Natural Science of China (61232014).

Originality/value – This paper presents a new topology optimization method for the optimal design of 2D and 3D porous materials for extreme elastic properties and macro-structural performance. Unlike previous studies, the presented paper tests the proposed optimization algorithm for not only 2D porous material design but also 3D topology optimization to reveal numerical and computational performance of the used algorithm. In addition, some new and interesting material microstructural topologies have been obtained to provide wider possible solutions to the material design.

Keywords Bi-directional evolutionary structural optimization (BESO), Elastic modulus, Material design, Mean compliance, Strain energy method

Paper type Research paper

1. Introduction

Composites possess outstanding physical, mechanical and thermal properties such as low ratio of weight to strength, corrosion and thermal resistance and toughness. Porous material as a special composite material has been widely used in industry field. For instance, there are honeycomb-like materials which are used for lightweight structural components, and products such as coffee cups and the insulation of booster rockets for space shuttles exploit the lower thermal conductivity of foam (Gibson and Ashby, 1997). When these heterogeneous materials are used, one has to account its effective constitutive properties first so as to assess the structural responses. Homogenization method is the most commonly used approach to evaluate the effective constitutive parameters of the considered periodical material microstructures or representative unit cell (RUC). This theory is based on rigorous mathematical argument and its numerical implementation procedure is well described in Guedes and Kikuchi (1990). Hassani and Hinton (1998a, 1998b) developed a review of numerical homogenization procedure and its conjunction with topology optimization. With the rapid advancing of processing technologies, it provides extensive opportunities for tailoring material microstructures for extreme material properties. By means of inverse homogenization, the topology optimization has been applied for tailoring material RUC with prescribed constitutive properties (Sigmund, 1994), extreme thermal expansion coefficients (Sigmund and Torquato, 1997), extreme viscoelastic behavior (Andreassen and Jensen, 2014; Chen and Liu, 2014), maximum stiffness and fluid permeability (Guest and Prévost, 2006; Guest and Prévost, 2007) and recently hyper-elastic properties (Wang *et al.*, 2014), etc. (Paulino *et al.*, 2009; Zhou *et al.*, 2010; Wang *et al.*, 2014; Li *et al.*, 2016).

Note that another valid approach for accounting material constituent behavior is the strain energy method which is based on average-field theory. Hori and Nemat-Nasser (1999) showed that the average-field and the homogenization theory can yield essentially the same effective modulus and boundary-value problems, while the former approach is more concise and efficient comparatively. Zhang *et al.* (2007a, 2007b) presented the topology optimization of material microstructure by using strain energy-based method which showed advantages of higher computing efficiency and simplified programming. Recently, an energy-based homogenization approach is adapted to the design of materials which significantly simplifies the numerical implementation (Xia and Breitkopf, 2015a). However, no matter which kind of method is used, the obtained material microstructures which process the same material properties could have totally different topologies. In other words, there are many locally optimal solutions in material design using topology optimization and parameters such as the initial guess of design domain and the used optimization algorithm have major influence on final designs. Therefore, it is meaningful of using different method to material microstructural design to find a much wider range of possible solutions.

This paper is an attempt to employ the strain energy method and the bi-directional evolutionary structural optimization (BESO) method to tailor material microstructures so as to find the optimal topology with the selected objective functions. Huang *et al.* (2011) first used the BESO method to designing periodic microstructures of porous materials for maximum bulk and shear modulus. Comparing with the continuous density-based topology optimization method, the feature of the BESO method is using discrete variables so that the obtained structures are very clear and easily manufactured (Huang and Xie, 2007; Huang and Xie, 2010a; Huang *et al.*, 2010; Huang and Xie, 2010b; Da *et al.*, 2017; Xia *et al.*, 2016). By BESO, some other extraordinary material properties, e.g. extreme electromagnetic permeability and permittivity (Huang *et al.*, 2012) and viscoelastic behavior (Huang *et al.*, 2015) were investigated.

Unlike the pure material design as aforementioned, design of a universal material microstructure for a fixed macrostructure was also investigated. Fujii *et al.* (2001) designed the composite materials that minimize the mean compliance of the macrostructure subject to volume fraction constraints of constituent phases. Huang *et al.* (2013) introduced a topology optimization algorithm for design of porous materials and composites so that the resulting macrostructure has the maximum stiffness. To reveal the equivalence of the solutions from the macro and micro approaches, Zuo *et al.* (2013) compared optimal material microstructures with optimal periodic structures. Xia and Breitkopf (2014b, 2014a, 2016, 2015b) addressed concurrent design of material and structure within the FE^2 nonlinear multi- scale analysis framework. However, these studies mainly focus on the optimal design of 2D porous or composite materials. The aims of this work are to integrate the established BESO method, stain energy method and material interpolation scheme to carry out not only the pure material design for maximum effective elastic modulus (bulk or shear modulus) but also the two-scale optimization problem by tailoring the 2D and 3D microstructural architectures for macroscopic structural compliance. The remainder of this paper is organized as follows: details of the stain energy-based method and sensitivity analysis are described in Section 2. Section 3 formulates pure material design for maximizing effective bulk modulus or shear modulus. Design of porous materials for the macro-structural stiffness is presented in Section 4. Concluding remarks are given in Section 5.

2. Principle of the stain energy-based method and sensitivity analysis

When a porous material is composed of RUCs periodically, the effective elasticity properties of this porous material can be calculated by the strain energy-based method. In this method, unit test strain ε_{ij}^0 imposes only on the boundaries of the RUC, and it satisfies the average strain theorem for elastic bodies (Zhang *et al.*, 2007b; Hashin, 1983): $\overline{\varepsilon_{ij}} = \varepsilon_{ij}^0$, where ε_{ij}^0 are constant strains.

The average strain and stress follow the linearity relation:

$$\overline{\boldsymbol{\sigma}_{ij}} = \boldsymbol{D}_{ijkl}^H \overline{\boldsymbol{\varepsilon}_{kl}} \tag{1}$$

where $\boldsymbol{D}_{ijkl}^H$ is the effective elastic modulus.

The strain energies stored in the RUC can be written as:

$$C = \frac{1}{2} \boldsymbol{D}_{ijkl}^H \overline{\boldsymbol{\varepsilon}_{ij}}\, \overline{\boldsymbol{\varepsilon}_{kl}} V \tag{2}$$

where V denotes the volume of the RUC.

For 2D orthotropic materials, the effective elastic matrix is formulated as equation (3). Four constant strains $\bar{\boldsymbol{\varepsilon}}^1 = (1\ 0\ 0)^T$, $\bar{\boldsymbol{\varepsilon}}^2 = (0\ 1\ 0)^T$, $\bar{\boldsymbol{\varepsilon}}^3 = (0\ 0\ 1)^T$ and $\bar{\boldsymbol{\varepsilon}}^4 = (1\ 1\ 0)^T$ are used to calculate four components of the effective elastic matrix. In the first test, suppose the average strain of the RUC is $\bar{\boldsymbol{\varepsilon}}^1 = (1\ 0\ 0)^T$, the average stress is $\bar{\boldsymbol{\sigma}}^1 = \left(\boldsymbol{D}^H_{1111}\ \boldsymbol{D}^H_{1122}\ 0\right)^T$ correspondingly. Then, the parameter $\boldsymbol{D}^H_{1111}$ can be calculated as: $\boldsymbol{D}^H_{1111} = 2C^1$, where C^1 denotes the strain energy of the first test (Zhang *et al.*, 2007b). It is seen that the remaining components of the $\boldsymbol{D}^H$ can be obtained through other three different test strain fields. The extension of computation of the effective elastic modulus to 3D is straightforward.

$$\boldsymbol{D}^H = \begin{bmatrix} \boldsymbol{D}^H_{1111} & \boldsymbol{D}^H_{1122} & 0 \\ & \boldsymbol{D}^H_{2222} & 0 \\ sym & & \boldsymbol{D}^H_{1212} \end{bmatrix} \tag{3}$$

Material interpolation scheme with penalization which has been widely used in the SIMP method by Bendsøe and Sigmund (1999) is adopted here to derive the sensitivities of the effective properties respect to the design variable:

$$\boldsymbol{K}(x_n) = \boldsymbol{K}_0(x_n)^P \tag{4}$$

where $\boldsymbol{K}_0$ indicates the stiffness matrix of solid elements. $\boldsymbol{K}(x_n)$ and x_n are the stiffness matrix and the relative density of an arbitrary element n, respectively. x_n is equal to 0.001 or 1 representing a void element or solid element, respectively. P is the penalty exponent and equals to 3 throughout this paper.

The finite element equilibrium equation of the RUC is:

$$\boldsymbol{KU} = \boldsymbol{F} \tag{5}$$

where $\boldsymbol{U}$ and $\boldsymbol{F}$ are the displacement vector and force vector respectively. $\boldsymbol{K}$ is the global stiffness matrix which is assembled by $\boldsymbol{K}(x_n)$.

Thus, the sensitivity of the strain energy with respect to the design variable x_n can be expressed as:

$$\frac{dC}{dx_n} = \frac{1}{2}\boldsymbol{U}^T\frac{\partial \boldsymbol{K}}{\partial x_n}\boldsymbol{U} = \frac{1}{2}P(\boldsymbol{U}_n)^T(x_n)^{P-1}\boldsymbol{K}_0\boldsymbol{U}_n = \frac{P}{x_n}C_n \tag{6}$$

It is observed from equation (6) that the sensitivity of the strain energy or effective elastic modulus with respect to design variables only depends on the element relative density and the strain energy. Therefore, the used strain energy-based method is relatively concise and extremely convenient for programming. In addition, it is straightforward to incorporate it with topological design of porous materials or composites for extreme material properties and macro-structural performance.

3. Topological design of materials for extreme properties

3.1 Optimization problem

It is well known that effective properties of composite materials are greatly depended on microscopic structural architecture/topology. To obtain heterogeneous materials with extreme properties, the goal, put simply, is to find an optimal material layout within the given domain (i.e. RUC in material design) for specified boundary conditions and constraints. Therefore, the topology optimization problem of porous materials for extreme elastic modulus can be mathematically written as:

$$\text{Maximize: } \psi = \omega_{ijkl} D^H_{ijkl} \tag{7}$$

$$\text{Subject to: } V(x) = \sum_{n=1}^{N} V_n x_n \tag{8}$$

$$x_n = 0.001 \; or \; 1, \cdots n = 1, 2, \ldots, N \tag{9}$$

where $V(x)$ denotes the objective volume of solid materials and V_n denotes the volume of the n-th element in the RUC. Binary design variable x_n is the relative density of the n-th element, where $x_n = 1x_n = 1$ indicates that the element is filled with solid materials and $x_n = 0.001$ means a void element. ω_{ijkl} is the weight factor and different objectives can be defined when ω_{ijkl} takes different values. For example, in 2D cases, the maximization of the material bulk modulus corresponds to the objective function $\psi = \frac{1}{4}\left(D^H_{1111} + D^H_{1122} + D^H_{2211} + D^H_{2222}\right)$ and the maximization of material shear modulus corresponds $\psi = D^H_{1212}$. Using equation (6), the sensitivity information of the selected objective function with respect to design variables can be calculated correspondingly.

3.2 Numerical implementation and optimization procedure

In this work, BESO algorithm is used to inversely optimize the topology of the material RUC. To conquer the common issues of structural topology optimization like checkerboard pattern and mesh-dependency, the n-th elemental sensitivity number is modified as Huang and Xie (2007):

$$\alpha_n = \frac{\sum_{m=1}^{M} \omega_{nm} \alpha_m}{\sum_{m=1}^{M} \omega_{nm}} \tag{10}$$

where α_n and α_m are, respectively, the sensitivity number of $n-$ and $m-$ element. ω_{nm} is a linear weight factor:

$$\omega_{nm} = \max\left(0, r_{min} - \Delta(n, m)\right) \tag{11}$$

determined according to the prescribed filter radius r_{min} and the center-center distance between elements n and m. To control the element sensitivity variation and improve the convergence of the proposed algorithm, the elemental sensitivity will be averaged with value of the previous iteration step. The cycle of finite element analysis and topological update continue until the target volume $V(x)$ is reached and the following convergence criterion in terms of objective values is satisfied.

$$\frac{\left|\left(\sum_{q=1}^{Q}\left(c_{l-q+1} - c_{l-Q-q+1}\right)\right)\right|}{\sum_{q=1}^{Q} c_{l-q+1}} \leq \tau \tag{12}$$

where l is the current iteration number, Q is the integral number and set to be 5 in this work, and τ is allowable convergence errors which is set to be 0.1 per cent. Thus, equation (12) means stable objective function in at least ten successive iterations. The whole optimization procedure for designing the microstructure of porous materials for extreme elastic properties is illustrated as Figure 1.

3.3 Numerical examples

In this section, several 2D and 3D numerical examples of pure material design for maximizing effective bulk or shear modulus are presented. It is assumed that the solid material with Young's modulus E = 1 and Poisson's ratio μ = 0.3 in both 2D and 3D examples. The RUC is discretized into 100 × 100 four-node quadrilateral (Q4) elements for 2D examples and 26 × 26 × 26 brick elements (C3D8 in ABAQUS) for 3D examples.

3.3.1 2D example for maximizing the shear modulus. The objective function of this example is to maximize the shear modulus of 2D porous materials. Three different initial designs of the RUC as shown in Figure 2 are considered. Initial design A is full with solid materials except four center elements, and initial design B is full with solid materials except for four corner elements and initial design C with eight elements at mid-sides of RUC for soft phase. Volume fractions of solid materials are set to 50 per cent in all three cases.

Figure 3 shows three final topologies of material RUC and their corresponding effective elasticity matrixes obtained from different initial designs. It is seen that soft phases are separated by the surrounding solid materials to maximize the effective shear modulus. The effective shear moduli for these three microstructures are 0.1394, 0.1392 and 0.1394. They

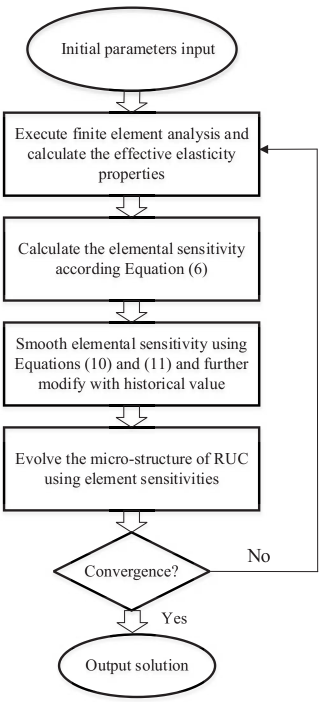

Figure 1.
Flowchart of materials design for extreme elastic properties

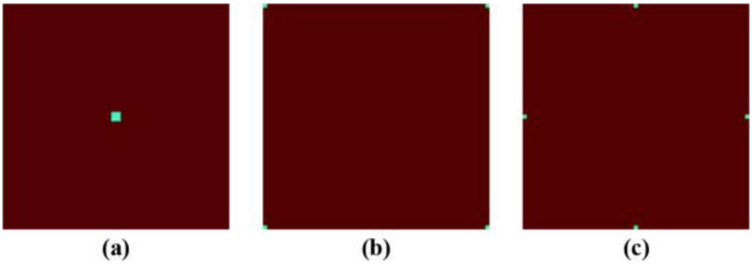

Figure 2. Initial designs

Notes: (a) Initial design A; (b) initial design B; (c) initial design C

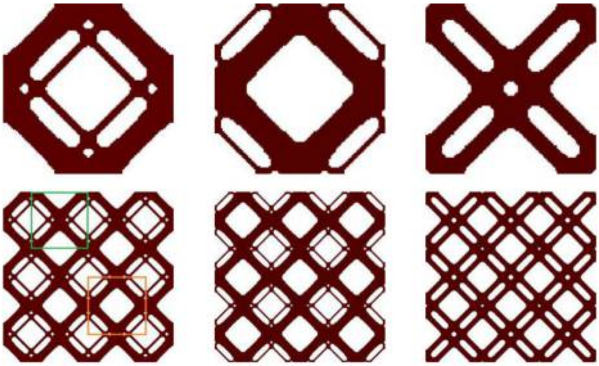

$$\begin{bmatrix} 0.1969 & 0.1657 & 0 \\ 0.1657 & 0.1969 & 0 \\ 0 & 0 & 0.1394 \end{bmatrix} \quad \begin{bmatrix} 0.1972 & 0.1632 & 0 \\ 0.1632 & 0.1972 & 0 \\ 0 & 0 & 0.1392 \end{bmatrix} \quad \begin{bmatrix} 0.1948 & 0.1705 & 0 \\ 0.1705 & 0.1948 & 0 \\ 0 & 0 & 0.1394 \end{bmatrix}$$

(a) (b) (c)

Figure 3. Microstructures and effective elasticity matrices of 2D porous materials with maximum shear modulus

Notes: (a) The resulted RUC from initial design A (above), 3×3 RUCs (middle) and effective elasticity matrix (below); (b) the resulted RUC from initial design B (above), 3×3 RUCs (middle) and effective elasticity matrix (below); (c) the resulted RUC from initial design C (above), 3×3 RUCs (middle) and effective elasticity matrix (below)

are very close to each other even though their topological configurations seem totally different. In fact, topologies shown in Figure 3(a) and (b) are identical if the RUC extends towards horizontal and vertical direction periodically. In other words, the RUC shown in Figure 3(b) obtained from initial design B is the same as the structure inside the orange square box in Figure 3(a) (middle). Furthermore, the resulting RUC obtained from initial design C is similar with the structure inside the green square box in Figure 3(a). The results are consistent with the knowledge in inverse homogenization design that different topologies of the RUC can possess the same effective elasticity property, and the initial design of the RUC effects the final result. Figure 4 plots the iteration process of shear modulus and volume fraction of solid phases within the RUC starting three different initial

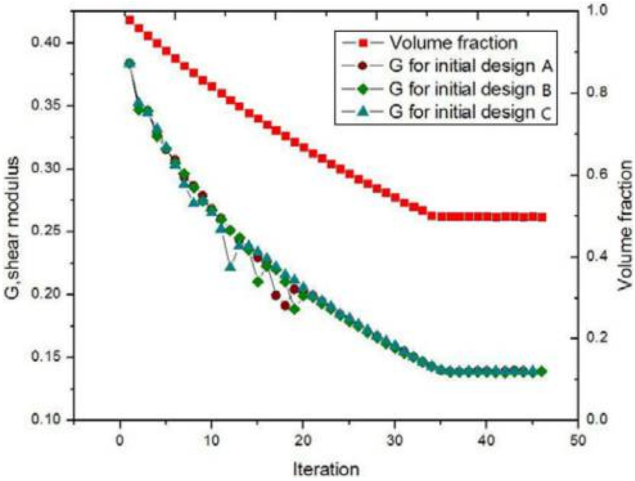

Figure 4.
Iterative process of shear modulus and volume fraction of solid materials for maximizing shear modulus of 2D porous materials

guesses. As can be seen, the evolution histories of the shear modulus starting from initial design A, B and C are very similar. The total iterations are 44, 45 and 46 which indicates that the proposed topology optimization method has good stability and high computational efficiency.

3.3.2 2D example for maximizing the bulk modulus. In this section, the optimization objective is selected as the bulk modulus of 2D porous materials, and the initial design A as shown in Figure 2 is used. Figure 5 shows the final microstructures and the corresponding effective elasticity matrixes when volume constrains of solid materials are set to be 60, 50, 40 and 30 per cent. The fan-like topologies are generated with the reduction of volume fraction of solid materials. The total iterations are 40, 49, 58 and 70 and the bulk moduli are 0.2396, 0.1796, 0.1304, and 0.0891. The Hashin–Shtrikman (HS) bounds (Hashin and Shtrikman, 1963) can be used to predict the maximum and minimum effective properties that a composite material could achieve. As for the porous materials, the void phase properties are equal to zero and the upper bound of bulk modulus can be Torquato *et al.* (1998):

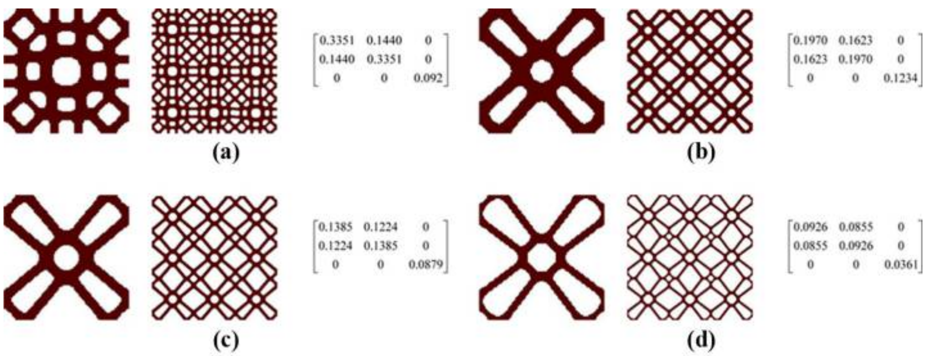

Notes: (a) 60%; (b) 50%; (c) 40%; (d) 30%

Figure 5.
RUC, 3 × 3 RUCs and Effective elasticity matrices of 2D porous materials with maximum bulk modulus for different volume fractions

$$K^* \leq \frac{V_f K^S G^S}{(1 - V_f)K^S + G^S} \tag{13}$$

where K^S and G^S are the bulk and shear modulus of solid materials respectively. K^* is the bulk modulus of the considered porous material and V_f is the volume fraction of solid phases of the porous material. Figure 6 draws the curve of the HS upper bound as the volume fraction of solid phase which shows a good agreement with the present solutions.

3.3.3 3D example for maximizing the shear modulus. In the following example, the optimization objective is to maximize the effective shear modulus of 3D porous materials. The optimization procedure starts from an initial design which is fully composed of solid materials except for eight center elements of the representative cubic cell. Figure 7 shows the final RUC, $2 \times 2 \times 2$ RUCs and effective elasticity matrixes when the volume constraints are set to be 35, 25 and 15 per cent, respectively. As can be observed, cross sections of obtained 3D microstructures are similar with the 2D microstructures in Section 3.3.1. The corresponding effective shear moduli are 0.0664, 0.0387 and 0.0164 and the total iterations are 41, 51 and 54, respectively. It is worthwhile noting that the iteration numbers are all less than 55 even though the volume constraint is as low as 15 per cent. Figure 8 shows iteration processes of volume fraction and effective shear modulus for the volume constraint 15 per cent.

3.3.4 3D example for maximizing the bulk modulus. Topological design of 3D porous materials for the bulk modulus is considered here. The optimization process starts from the initial design where eight elements at the corner of cubic unit cell are assigned as void element. The volume fractions of solid materials are set to be 55, 35 and 15 per cent of the whole design domain. The final microstructural topologies of the RUC and their $2 \times 2 \times 2$ RUCs and effective elasticity matrixes are shown in Figure 9. The total iterations are 42, 40 and 66, and the final bulk moduli are 0.2551, 0.1192 and 0.0265. As in the previous examples,

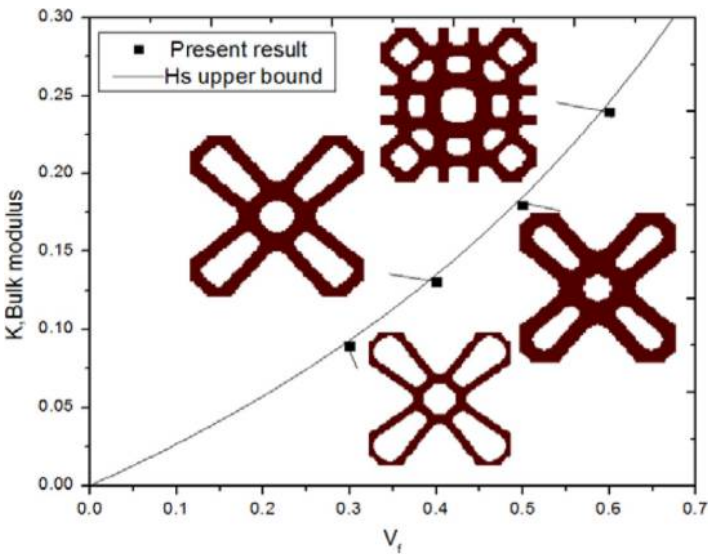

Figure 6.
Comparison between the present solutions and HS bounds

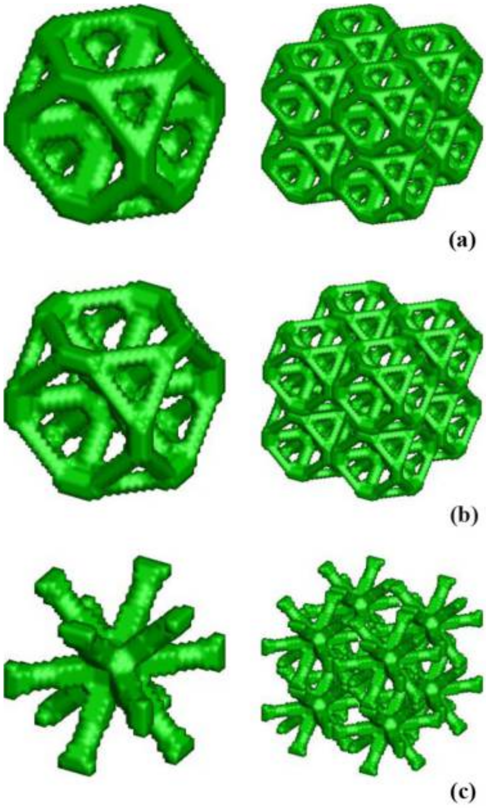

$$\begin{bmatrix} 0.1468 & 0.0711 & 0.0711 & 0 & 0 & 0 \\ 0.0711 & 0.1468 & 0.0711 & 0 & 0 & 0 \\ 0.0711 & 0.0711 & 0.1468 & 0 & 0 & 0 \\ 0 & 0 & 0 & 0.0664 & 0 & 0 \\ 0 & 0 & 0 & 0 & 0.0664 & 0 \\ 0 & 0 & 0 & 0 & 0 & 0.0664 \end{bmatrix}$$

$$\begin{bmatrix} 0.0854 & 0.0426 & 0.0426 & 0 & 0 & 0 \\ 0.0426 & 0.0854 & 0.0426 & 0 & 0 & 0 \\ 0.0426 & 0.0426 & 0.0854 & 0 & 0 & 0 \\ 0 & 0 & 0 & 0.0387 & 0 & 0 \\ 0 & 0 & 0 & 0 & 0.0387 & 0 \\ 0 & 0 & 0 & 0 & 0 & 0.0387 \end{bmatrix}$$

$$\begin{bmatrix} 0.0388 & 0.0183 & 0.0183 & 0 & 0 & 0 \\ 0.0183 & 0.0388 & 0.0183 & 0 & 0 & 0 \\ 0.0183 & 0.0183 & 0.0388 & 0 & 0 & 0 \\ 0 & 0 & 0 & 0.0164 & 0 & 0 \\ 0 & 0 & 0 & 0 & 0.0164 & 0 \\ 0 & 0 & 0 & 0 & 0 & 0.0164 \end{bmatrix}$$

Notes: (a) 35%; (b) 25%; (c) 15%

Figure 7.
RUC, $2 \times 2 \times 2$ RUCs and Effective elasticity matrices of 3D porous materials with maximum shear modulus for different volume fractions

the microstructural topologies keep consistency with the decrease of the volume fraction of solid materials.

4. Topological design of materials for macrostructures

4.1 Optimization problem and sensitivity analysis

This section describes the optimal design of porous materials to minimize the mean compliance of the considered macrostructures. Figure 10 illustrates a macrostructure composed of porous materials with periodic microstructures. The microstructures are very small compared with the characteristic dimension of the macrostructure. For such a two-scale topology optimization problem, there are two types of finite element models, i.e. one is the micro model for the microstructure RUC which is served as the design domain, and the other is the macro model with respect to the macrostructure for calculating the macroscopic structural response. The mathematical formulation of design of material microstructures for the fixed macrostructure with maximum stiffness reads as follows:

$$\text{Minimize}: c = \frac{1}{2} \boldsymbol{U}^T \boldsymbol{K} \boldsymbol{U} \tag{14}$$

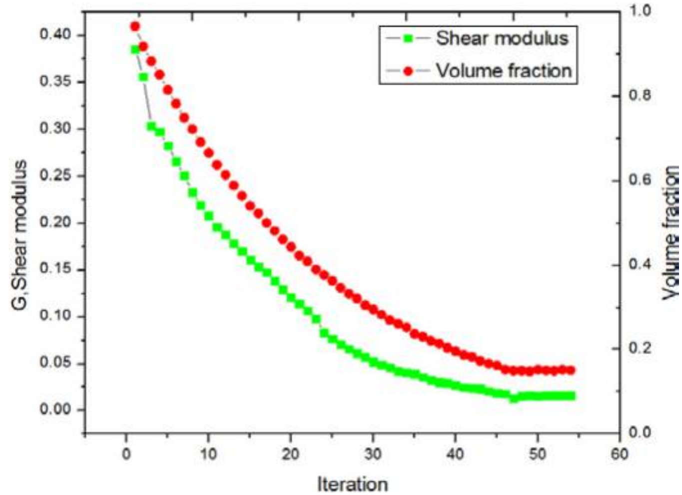

Figure 8.
Iterative process of shear modulus and volume fraction of solid materials for maximizing shear modulus of 3D porous materials

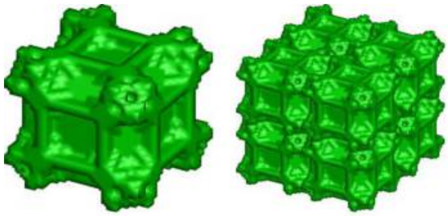

$$\begin{bmatrix} 0.4710 & 0.1472 & 0.1472 & 0 & 0 & 0 \\ 0.1472 & 0.4710 & 0.1472 & 0 & 0 & 0 \\ 0.1472 & 0.1472 & 0.4710 & 0 & 0 & 0 \\ 0 & 0 & 0 & 0.1211 & 0 & 0 \\ 0 & 0 & 0 & 0 & 0.1211 & 0 \\ 0 & 0 & 0 & 0 & 0 & 0.1211 \end{bmatrix}$$

(a)

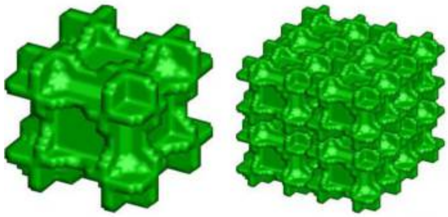

$$\begin{bmatrix} 0.2333 & 0.0623 & 0.0623 & 0 & 0 & 0 \\ 0.0623 & 0.2333 & 0.0623 & 0 & 0 & 0 \\ 0.0623 & 0.0623 & 0.2333 & 0 & 0 & 0 \\ 0 & 0 & 0 & 0.0529 & 0 & 0 \\ 0 & 0 & 0 & 0 & 0.0529 & 0 \\ 0 & 0 & 0 & 0 & 0 & 0.0529 \end{bmatrix}$$

(b)

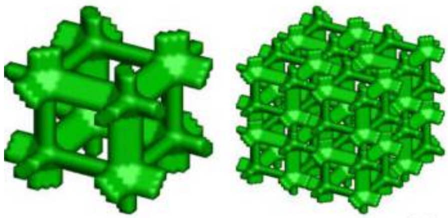

$$\begin{bmatrix} 0.0669 & 0.0063 & 0.0063 & 0 & 0 & 0 \\ 0.0063 & 0.0669 & 0.0063 & 0 & 0 & 0 \\ 0.0063 & 0.0063 & 0.0669 & 0 & 0 & 0 \\ 0 & 0 & 0 & 0.0030 & 0 & 0 \\ 0 & 0 & 0 & 0 & 0.0030 & 0 \\ 0 & 0 & 0 & 0 & 0 & 0.0030 \end{bmatrix}$$

(c)

Notes: (a) 55%; (b) 35%; (c) 15%

Figure 9.
RUC, 2 × 2 × 2 RUCs and Effective elasticity matrices of 3D porous materials with maximum bulk modulus for different volume fractions

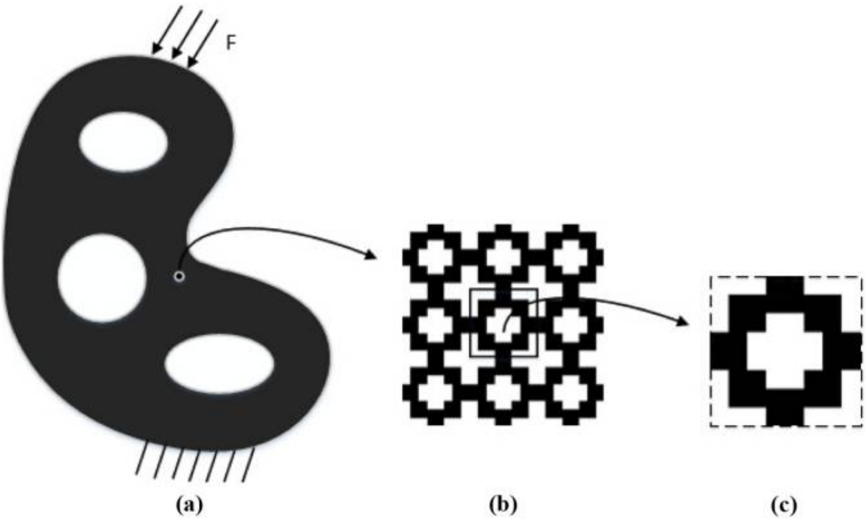

Notes: (a) macrostructure; (b) RUCs; (c) RUC

Figure 10. A Macrostructure composed of porous materials

$$\text{Subject to}: V_x - \frac{\sum_{m=1}^{M}\sum_{n=1}^{N} x_n V_n}{\sum_{m=1}^{M}\sum_{n=1}^{N} V_n} = 0 \tag{15}$$

$$\boldsymbol{KU} = \boldsymbol{F} \tag{16}$$

$$x_n = 0.001 \; or \; 1 \cdots n = 1, 2, \ldots, N \tag{17}$$

where c denotes the mean compliance of the considered macrostructure. M and N denote the total number of elements in the macro and micro finite element models, respectively. V_n is the volume of the n-th element in the RUC and V_x is the final volume fraction of solid materials. The binary variable x_n denotes the relative density of the n-th element in the micro model. $\boldsymbol{F}$ and $\boldsymbol{U}$ are the force vector and the global displacement vector in the macro model, respectively. $\boldsymbol{K}$ is the global stiffness matrix of the macrostructure which is obtained by assembling the element stiffness matrices, $\boldsymbol{K}_m$:

$$\boldsymbol{K}_m = \int_{V_m} \boldsymbol{B}\boldsymbol{D}^H \boldsymbol{B} dV_m \tag{18}$$

where $\boldsymbol{B}$ is the strain-displacement matrix. V_m denotes the volume of the m-th element in the macro model. $\boldsymbol{D}^H$ is the effective elastic matrix which should be computed form the finite element analysis of RUC using the strain energy-based method. Thus, the material elasticity property is embedded in the macro-scale finite element analysis from equation (18).

Sensitivity information is indispensable for determining the evolutionary strategy in the BESO method. The derivative of the macroscopic structural mean compliance with respect to the design variable in the micro model can be expressed as:

$$\frac{dc}{dx_n} = -\frac{1}{2}\sum_{m=1}^{M} \boldsymbol{U}_m^T \frac{\partial \boldsymbol{K}_m}{\partial x_n} \boldsymbol{U}_m = -\frac{1}{2}\sum_{m=1}^{M} \boldsymbol{U}_m^T \int_{V_m} \boldsymbol{B}^T \frac{\partial \boldsymbol{D}^H}{\partial x_n} \boldsymbol{B} dV_m U_m \tag{19}$$

Therefore, the sensitivity information of micro-scale analysis is coupled with the displacement field of the macrostructure. In addition, it is noted that the gradient information of the D^H with respect to the design variable x_n in equation (19) can be directly obtained according to equation (6). The way of sensitivity calculation in regard to micro variable shows that the strain energy-based is very suitable for solving this two-scale topology optimization problem.

4.2 Numerical implementation and optimization procedure

As mentioned in Section 3.2, the mesh-independent filter formulated in equations (10) and (11) which aims to overcome some common numerical issues like checkerboard pattern is used here. The flowchart of the numerical implementation of design of porous material for macroscopic structural stiffness is given in Figure 11. The convergence criterion formulated in equation (12) is also adopted to stop the optimization iteration. In this two-scale optimization problem, the effective properties of porous materials are obtained via strain energy-base method which serves as a bridge of the finite element models of macrostructure

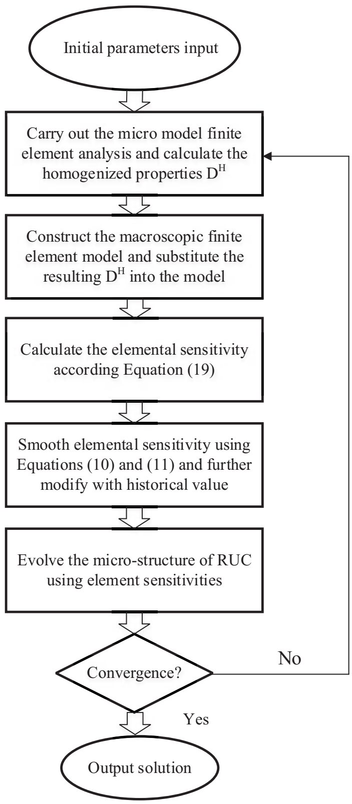

Figure 11.
Flowchart of materials design for macrostructures

and material microstructures. The topologies of material microstructures are inversely optimized based on BESO approach. The optimization process is terminated while both volume constraint and convergence criterion are satisfied.

4.3 Numerical examples

4.3.1 2D example. It is assumed that the 2D cantilever as shown in Figure 12 is composed of periodic porous materials. The objective is to tailor material microstructures for the fixed cantilever with minimum macroscopic structural compliance by limiting the volume of material. The solid material of an element in the material RUC is assumed to be isotropic with Young's modulus $E = 1$ and Poisson's ratio $\mu = 0.3$, and volume constraint is set to be 40 per cent of the design domain. The square RUC is discretized into 100×100 four-node quadrilateral (Q4) elements.

To start the optimization process, the two initial designs shown in Figure 2(a) and (b) are used. For the cantilever with different L and H values, the optimized microstructures of porous materials and their effective elasticity properties starting from two initial guesses are demonstrated in Figure 13. As can be observed, the obtained topologies are completely different with those in Section 3.3. In addition, the effective constitutive matrices starting from initial B are very close to that starting from initial A, even though the microstructural topologies seem different. Once again, it verifies the fact that different microstructures could hold the same elastic property. Furthermore, the final mean compliance of the cantilever beam with $L = 20$, $H = 40$ are 25.3817 and 25.4046 when the optimization procedure starting from initial designs A and B, respectively. They are very close to each other, and it can therefore be concluded that different material microstructural topologies could result same macroscopic structural stiffness.

4.3.2 3D example. A 3D cantilever under a point load is given here to further demonstrate the presented optimization approach. Figure 14 shows the 3D cantilever which is composed of porous materials with periodic microstructures. The optimization objective is to find the best distribution of a certain amount of solid materials within the RUC so that the macroscopic cantilever has the maximum structural stiffness. It is assumed that the solid material of an element in the material RUC is isotropic with Young's modulus $E = 1$ and Poisson's ratio $\mu = 0.3$, and the volume fraction of solid materials is set to 60 per cent.

The cubic RUC which serves as the design domain is small enough compared with the macrostructure, and it is discretized into $26 \times 26 \times 26$ brick elements (C3D8 in ABAQUS). The whole optimization procedure starts from the initial design which is fully occupied by solid materials except for eight corner elements for void phase. The resulting RUC, $2 \times 2 \times 2$ RUCs and effective elasticity matrixes for the 3D cantilever with different values of L, H and B are shown in Figure 15. The final topologies are completely different with change of the

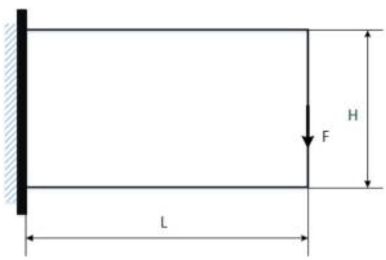

Figure 12.
A 2D Cantilever with length L and height H

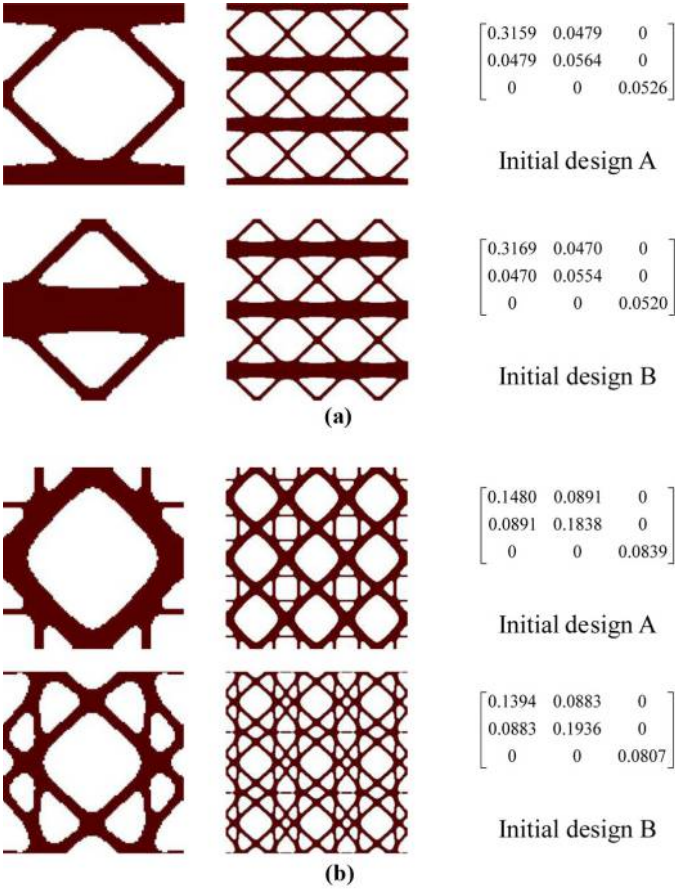

Notes: (a) $L = 40$ and $H = 20$; (b) $L = 20$ and $H = 40$

Figure 13.
RUC, 3 × 3 RUCs and Effective elasticity matrices of 2D porous materials starting from different initial design for cantilevers with L and H

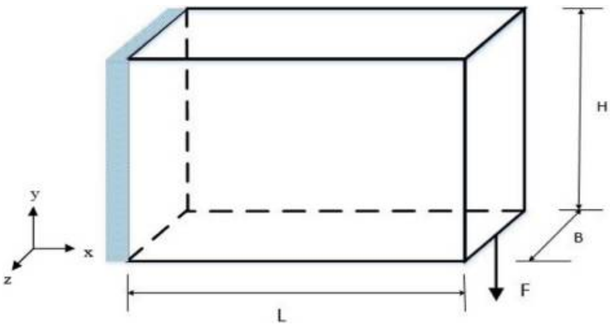

Figure 14.
A 3D Cantilever with length L, width B and height H

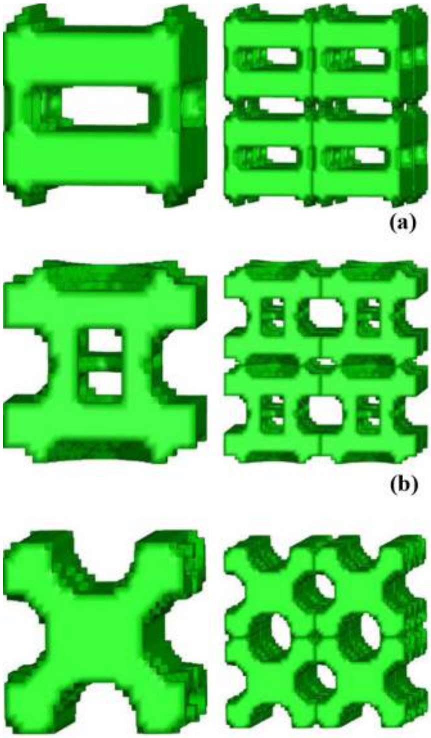

0.6301	0.0311	0.1977	0	0	0
0.0311	0.0904	0.0404	0	0	0
0.1977	0.0404	0.6527	0	0	0
0	0	0	0.0182	0	0
0	0	0	0	0.0396	0
0	0	0	0	0	0.2190

(a)

0.5215	0.1053	0.1866	0	0	0
0.1053	0.3261	0.132	0	0	0
0.1866	0.132	0.6661	0	0	0
0	0	0	0.0580	0	0
0	0	0	0	0.1318	0
0	0	0	0	0	0.1829

(b)

0.3361	0.1875	0.1557	0	0	0
0.1875	0.3677	0.1657	0	0	0
0.1557	0.1657	0.6762	0	0	0
0	0	0	0.1130	0	0
0	0	0	0	0.1620	0
0	0	0	0	0	0.1436

(c)

Notes: (a) $L = 20$, $H = 20$ and $B = 10$; (b) $L = 20$, $H = 10$ and $B = 20$; (c) $L = 10$, $H = 20$ and $B = 20$

Figure 15.
RUC, $2 \times 2 \times 2$ RUCs and Effective elasticity matrices for 3D cantilever with L, H and B

size of the macrostructure itself. It should be noted that the solutions of material microstructures for the 3D macroscopic cantilever is not unique because it also depends on the selection of the initial design of RUC.

5. Conclusions

In this paper, the microstructural topologies of porous materials are tailored for extreme effective elastic modulus and for macroscopic structural stiffness. The adoption of the strain energy-based method simplifies the numerical implementation. The BESO approach is adopted to the inverse design of porous materials, and the generated topologies are described clearly which makes it easy to manufacture. Several 2D and 3D numerical examples show that the presented method has high stability and requires little iterations for convergence. In addition, numerical examples consider the effect of initial guesses of design domain and of volume constraint of solid materials on the final design. Some interesting microstructural topologies of porous materials for the maximum bulk modulus or shear modulus are generated. Furthermore, the presented method is extended to tailor the microstructures of porous materials so that the macroscopic structures have the minimum mean compliance. The optimal result depends on various effects such as the initial guess of RUC and the size dimension of the macrostructure itself. It is worth mentioning that the extension of the presented method to optimal design of multi-phase composite materials or concurrent topological design of materials and structures is straightforward.

References

Andreassen, E. and Jensen, J. (2014), "Topology optimization of periodic microstructures for enhanced dynamic properties of viscoelastic composite materials", *Structural and Multidisciplinary Optimization*, Vol. 49 No. 5, pp. 695-705.

Bendsøe, M.P. and Sigmund, O. (1999), "Material interpolations in topology optimization", *Archive of Applied Mechanics*, Vol. 69 Nos 9/10, pp. 635-654.

Chen, W. and Liu, S. (2014), "Topology optimization of microstructures of viscoelastic damping materials for a prescribed shear modulus", *Structural and Multidisciplinary Optimization*, Vol. 50 No. 2, pp. 287-296.

Da, D.C., Cui, X.Y., Long, K. and Li, G.Y. (2017), "Concurrent topological design of composite structures and the underlying multi-phase materials", *Computers & Structures*, Vol. 179, pp. 1-14.

Fujii, D., Chen, B.C. and Kikuchi, N. (2001), "Composite material design of two-dimensional structure using the homogenization design method", *International Journal for Numerical Methods in Engineering*, Vol. 50 No. 9, pp. 2031-2051.

Gibson, L.J. and Ashby, M.F. (1997), *Cellular Solids: Structure and Properties*, Cambridge University Press, Cambridge.

Guedes, J. and Kikuchi, N. (1990), "Preprocessing and postprocessing for materials based on the homogenization method with adaptive finite element method", *Computer Methods in Applied Mechanics and Engineering*, Vol. 83 No. 2, pp. 143-198.

Guest, J.K. and Prévost, J.H. (2006), "Optimizing multifunctional materials: Design of microstructures for maximized stiffness and fluid permeability", *International Journal of Solids and Structures*, Vol. 43 No. 22-23, pp. 7028-7047.

Guest, J.K. and Prévost, J.H. (2007), "Design of maximum permeability material structures", *Computer Methods in Applied Mechanics and Engineering*, Vol. 196 Nos 4/6, pp. 1006-1017.

Hashin, Z. (1983), "Analysis of composite materials – a survey", *Journal of Applied Mechanics*, Vol. 50 No. 3, pp. 481-505.

Hashin, Z. and Shtrikman, S. (1963), "Avariational approach to the theory of the elastic behaviour of multiphase materials", *Journal of Physics and Chemistry of Solids*, Vol. 11 No. 2, pp. 127-140.

Hassani, B. and Hinton, E.A. (1998a), "Review of homogenization and topology optimization I-homogenization for media with periodic structure", *Computers & Structures*, Vol. 69, pp. 707-717.

Hassani, B. and Hinton, E.A. (1998b), "Review of homogenization and topology optimization II-analytical and numerical solution of homogenization equations", *Computers & Structures*, Vol. 69, pp. 719-738.

Hori, M. and Nemat-Nasser, S. (1999), "Two micromechanics theories for determining micro ± macro relations in heterogeneous solids", *Mechanics of Materials*, Vol. 31 No. 10, pp. 667-682.

Huang, X. and Xie, Y.M. (2007), "Convergent and mesh-independent solutions for the bi-directional evolutionary structural optimization method", *Finite Elements in Analysis and Design*, Vol. 43 No. 14, pp. 1039-1049.

Huang, X. and Xie, Y.M. (2010a), "A further review of eso type methods for topology optimization", *Structural and Multidisciplinary Optimization*, Vol. 41 No. 5, pp. 671-683.

Huang, X. and Xie, Y.M. (2010b), *Evolutionary Topology Optimization of Continuum Structures: methods and Applications*, John Wiley & Sons, Chichester.

Huang, X., Radman, A. and Xie, Y.M. (2011), "Topological design of microstructures of cellular materials for maximum bulk or shear modulus", *Computational Materials Science*, Vol. 50 No. 6, pp. 1861-1870.

Huang, X., Zuo, Z.H. and Xie, Y.M. (2010), "Evolutionary topological optimization of vibrating continuum structures for natural frequencies", *Computers & Structures*, Vol. 88 Nos 5/6, pp. 357-364.

Huang, X., Zhou, S., Xie, Y.M. and Li, Q. (2013), "Topology optimization of microstructures of cellular materials and composites for macrostructures", *Computational Materials Science*, Vol. 67, pp. 397-407.

Huang, X., Xie, Y.M., Jia, B., Li, Q. and Zhou, S.W. (2012), "Evolutionary topology optimization of periodic composites for extremal magnetic permeability and electrical permittivity", *Structural and Multidisciplinary Optimization*, Vol. 46 No. 3, pp. 385-398.

Huang, X., Zhou, S., Sun, G., Li, G.Y. and Xie, Y.M. (2015), "Topology optimization for microstructures of viscoelastic composite materials", *Computer Methods in Applied Mechanics and Engineering*, Vol. 283, pp. 503-516.

Li, H., Luo, Z., Zhang, N., Gao, L. and Brown, T. (2016), "Integrated design of cellular composites using a level-set topology optimization method", *Computer Methods in Applied Mechanics and Engineering*, Vol. 309, pp. 453-475.

Paulino, G.H., Silva, E.C.N. and Le, C.H. (2009), "Optimal design of periodic functionally graded composites with prescribed properties", *Structural and Multidisciplinary Optimization*, Vol. 38 No. 5, pp. 469-489.

Sigmund, O. (1994), "Materials with prescribed constitutive parameters: an inverse homogenization problem", *International Journal of Solids and Structures*, Vol. 31 No. 17, pp. 2313-2329.

Sigmund, O. and Torquato, S. (1997), "Design of materials with extreme thermal expansion using a three-phase topology optimization method", *Journal of the Mechanics and Physics of Solids*, Vol. 45 No. 6, pp. 1037-1067.

Torquato, S., Gibiansky, L.V., Silva, M.J. and Gibson, L.J. (1998), "Effective mechanical and transport properties of cellular solids", *International Journal of Mechanical Sciences*, Vol. 40 No. 1, pp. 71-82.

Wang, F., Sigmund, O. and Jensen, J. (2014), "Design of materials with prescribed nonlinear properties", *Journal of the Mechanics and Physics of Solids*, Vol. 69(, pp. 1):156-174.

Wang, Y., Luo, Z., Zhang, N. and Kang, Z. (2014), "Topological shape optimization of micro-structure metamaterials using a level set method", *Computational Materials Science*, Vol. 87, pp. 178-186.

Xia, L. and Breitkopf, P. (2014a), "A reduced multiscale model for nonlinear structural topology optimization", *Computer Methods in Applied Mechanics and Engineering*, Vol. 280, pp. 117-134.

Xia, L. and Breitkopf, P. (2014b), "Concurrent topology optimization design of material and structure within fe^2 nonlinear multiscale analysis framework", *Computer Methods in Applied Mechanics and Engineering*, Vol. 278, pp. 524-542.

Xia, L. and Breitkopf, P. (2015a), "Design of materials using topology optimization and energy-based homogenization approach in matlab", *Structural and Multidisciplinary Optimization*, Vol. 1.

Xia, L. and Breitkopf, P. (2015b), "Multiscale structural topology optimization with an approximate constitutive model for local material microstructure", *Computer Methods in Applied Mechanics and Engineering*, Vol. 286, pp. 147-167.

Xia, L. and Breitkopf, P. (2016), "Recent advances on topology optimization of multiscale nonlinear structures", *Archives of Computational Methods in Engineering*, Vol. 24 No. 2, doi: 10.1007/s11831-016-9170-7.

Xia, L., Xia, Q., Huang, X. and Xie, Y.M. (2016), "Bi-directional evolutionary structural optimization on advanced structures and materials: a comprehensive review", *Arch Computer Methods in Applied Mechanics and Engineering*, Vol. 1, doi: 10.1007/s11831-016-9203-2.

Zhang, W., Wang, F., Dai, G. and Sun, S. (2007a), "Topology optimal design of material microstructures using strain energy-based method", *Chinese Journal of Aeronautics*, Vol. 20, pp. 320-326.

Zhang, W., Dai, G., Wang, F., Sun, S. and Bassir, H. (2007b), "Using strain energy-based prediction of effective elastic properties in topology optimization of material microstructures", *AActa Mechanica Sinica/Lixue Xuebao*, Vol. 23 No. 1, pp. 77-89.

Zhou, S., Li, W., Sun, G. and Li, Q. (2010), "A level-set procedure for the design of electromagnetic metamaterials", *Optics Express*, Vol. 18 No. 7, pp. 6693-6702.

Zuo, Z., Huang, X., Yang, X., Rong, J. and Xie, Y.M. (2013), "Comparing optimal materials microstructures with optimal periodic structures", *Computational Materials Science*, Vol. 69, pp. 137-147.